

Attitude-Estimation-Free GNSS and IMU Integration

Taro Suzuki¹

Abstract—A global navigation satellite system (GNSS) is a sensor that can acquire 3D position and velocity in an earth-fixed coordinate system and is widely used for outdoor position estimation of robots and vehicles. Various GNSS/inertial measurement unit (IMU) integration methods have been proposed to improve the accuracy and availability of GNSS positioning. However, all of them require the addition of a 3D attitude to the estimated state in order to fuse the IMU data. This study proposes a new optimization-based positioning method for combining GNSS and IMU that does not require attitude estimation. The proposed method uses two types of constraints: one is a constraint between states using only the magnitude of the 3D acceleration observed by an accelerometer, and the other is a constraint on the angle between the velocity vectors using the amount of angular change by a gyroscope. The evaluation results with simulation data show that the proposed method maintains the position estimation accuracy even when the IMU mounting position error increases and improves the accuracy when the GNSS observations contain multipath errors or missing data. The proposed method could improve the positioning accuracy in experiments using IMUs acquired in real environments.

I. INTRODUCTION

The global navigation satellite system (GNSS), represented by GPS, has become an indispensable infrastructure in today's society as a means of estimating a location in outdoor environments. For example, it plays an important role in various applications such as the navigation of people and vehicles in cities, unmanned delivery robots, autonomous flight of drones, and automated driving of vehicles. However, GNSS alone is difficult to use for positioning in environments such as tunnels, under trees, and elevated structures where signals from GNSS satellites are blocked. In urban environments, GNSS signals are reflected or diffracted and enter the antenna, a phenomenon known as multipath, which greatly reduces positioning accuracy [1], [2]. As a result, several studies are being conducted to improve the availability and accuracy of GNSS [3].

One way to improve the availability and accuracy of GNSS in urban environments is to combine velocity with position estimation by using GNSS Doppler shift measurements. The 3D velocity in an earth-fixed coordinate system is estimated directly from GNSS Doppler measurements. 3D velocity can be estimated with cm/s level accuracy in an ideal open-sky environment, which is much higher than that calculated from GNSS pseudorange measurements [4]. In addition, Doppler is known to be more robust than GNSS pseudorange because it is resistant to multipath and instantaneous signal blocking [5]. However, when there is prolonged signal blocking or

when only reflected signals are incident on the antenna, the combined Doppler velocity is not expected to improve the accuracy of the position estimate.

Many studies have been conducted to combine GNSS and inertial measurement units (IMUs) to solve this problem [6]. Acceleration and angular velocity, IMU measurements, do not depend on the environment for measurement accuracy like GNSS signals. For this reason, GNSS and IMU are complementary, and combining the two improves the accuracy and availability of position estimation. Filtering methods, such as complementary filters [7] and Kalman filters (KFs) [6], and, more recently, optimization-based methods, such as graph optimization [8], are often used to combine GNSS and IMU.

However, GNSS/IMU integration has the following problems.

- IMU integration requires 3D attitude estimation, and even in applications where only position is required, it is necessary to solve the 6-DOF pose estimation problem.
- The position and attitude of the IMU relative to the vehicle frame must be rigorously measured or calibrated in advance; any error in the IMU mounting angle and position will degrade the position estimation accuracy after GNSS integration.

This study proposes a new GNSS/IMU integration method that does not require attitude estimation. We propose a state-to-state constraint using only the magnitude of the acceleration vector of the IMU output and a velocity vector direction constraint using an integration of angular velocities. Because the proposed method does not estimate 3D attitude, the effect of the IMU mounting angle and position on accuracy is small, and there is no need to calibrate. Therefore, the proposed method is effective for problems where sensors (e.g., smartphones) containing GNSS and IMU are mounted on a vehicle or robot in different positions and orientations each time and used for navigation. It can also simplify the system for navigation applications where only position is needed. In addition, the combined IMU can improve accuracy when GNSS Doppler observations are unavailable due to satellite shielding or when multipath errors are large.

A. Related Studies

Combining GNSS with other sensors has been studied extensively: GNSS combined with a camera [9], [10] and lidar [11], [12] has been proposed, but the most commonly used combination is with an IMU [6], [13]. This study uses a low-cost MEMS IMU consisting of a 3-axis accelerometer and a 3-axis gyroscope. Compared to GNSS, IMU has a high sampling rate (typically 100 to 200 Hz) and provides highly

¹Taro Suzuki is with Future Robotics Technology Center, Chiba Institute of Technology, Japan taro@furo.org

continuous acceleration and angular velocity measurements. Although the IMU can measure velocity and angular change by integrating its measurements, integration errors accumulate. Therefore, by combining IMU with GNSS, which has a low sampling rate but provides absolute position and velocity, error accumulation can be eliminated, and smooth position and attitude estimation are possible.

Classified in terms of combined GNSS and IMU methods, many of them use KFs [14], [15]. Complementary filter-based algorithms are often used in environments with more limited computational resources [7]. Recently, GNSS/IMU integration using optimization methods has also been studied [16]–[20]: in [17], [19], a method for integration GNSS pseudorange observations and IMU with tight coupling is proposed using pose graph optimization; in [17], [19], in addition to GNSS and IMU, time differences in carrier phase are integrated as precise velocity constraints. Compared to the method using KF, the method using optimization is reported to have an advantage in terms of accuracy [16], [21].

However, all of these methods add a 3D attitude to the state to be estimated. In order to decompose and apply the 3D acceleration measurements from the accelerometer to the navigation coordinate system, estimation of the 3D attitude is required. Reference [21] integrates the IMU without including attitude as a state, but 3D attitude is obtained directly from the attitude heading reference system (AHRS). Therefore, errors in the AHRS will affect the accuracy of the position estimate. Instead of estimating the attitude, reference [22] improves the accuracy of the position estimate by using the zero velocity observation at the constraint obtained from the IMU. However, this constraint only contributes when the vehicle is stationary.

In addition, the combination of GNSS and IMU requires a homogeneous transformation matrix from the IMU coordinate system to the vehicle coordinate system (vehicle center of rotation) [23]. In many cases, the IMU mounting angle and position with respect to the vehicle frame are accurately measured in advance, or the IMU mounting error is added to the estimated state and estimated simultaneously [24]. In cases where the IMUs are frequently removed and replaced, pre-measuring the IMU mounting angles and positions is time-consuming.

B. Contributions

The contributions of the proposed method are as follows.

- A new IMU constraint is proposed that does not require attitude estimation, and a combined GNSS/IMU method is developed that is independent of IMU mounted angle and position.
- The proposed method significantly improves position estimation accuracy in environments where GNSS velocity observations are unavailable or contain errors due to satellite shielding or multipath.
- Through simulations and real-world experiments, we compared the accuracy of the proposed method with that of the conventional 6-DOF pose estimation method,

which adds attitude to the estimated state. We clarified the applicability and effectiveness of the proposed method.

II. PROPOSED METHOD

A. Problem Setup

Generally, the 3D position \mathbf{x} and 3D attitude Φ are used as the estimated state in a combined GNSS and IMU system. In addition, the 3D velocity \mathbf{v} is estimated from the measured acceleration and angular velocity from the IMU. As low-cost IMUs have large acceleration and angular rate bias errors and their drifts, the biases of each of the 3-axes \mathbf{b}_{acc} and \mathbf{b}_{gyro} are often added to the state. In a general GNSS/IMU integration, the estimated state at i -th epoch is as follows.

$$\mathbf{X}_i = [\mathbf{x}_i \quad \Phi_i \quad \mathbf{v}_i \quad \mathbf{b}_{\text{acc},i} \quad \mathbf{b}_{\text{gyro},i}]^T \quad (1)$$

Here, the local east-north-up (ENU) coordinate system is adopted as the world frame. This is a 15-dimensional state estimation problem. The measured values of acceleration $\tilde{\mathbf{a}}$ and angular velocity $\tilde{\omega}$ of IMU in the IMU frame is follows.

$$\tilde{\mathbf{a}}_i = \mathbf{R}_{W,i}^T (\mathbf{a}_i - \mathbf{g}) + \mathbf{b}_{\text{acc},i} + \eta_{\text{acc}} \quad (2)$$

$$\tilde{\omega}_i = \omega_i + \mathbf{b}_{\text{gyro},i} + \eta_{\text{gyro},i} \quad (3)$$

where \mathbf{a} and ω are the theoretical values of acceleration and angular velocity, \mathbf{g} is the gravitational acceleration, η represent Gaussian white noise, and \mathbf{R}_W^T denotes the rotation matrix from the world frame to the IMU frame computed from 3D attitude Φ and IMU mounting angle in the vehicle frame.

As can be seen from equation (2), in order to combine the IMU observations with the GNSS observations in the world frame, it is necessary to estimate the 3D attitude Φ and IMU mounting angle, which represent a transformation from the IMU frame to the world frame. In addition, if the IMU mounting position is not aligned with the vehicle rotation center, the observed acceleration will include the additional centripetal force, and if the acceleration is not properly corrected using the IMU mounting position, errors in attitude estimation will occur [23].

B. Estimated State

In contrast, this study does not estimate the 3D attitude and the IMU mounting angle and position but combines the IMU and GNSS observation; the IMU and GNSS observations are exactly the same as in the conventional method, but the state is the following eight dimensions without attitude.

$$\mathbf{X}_i = [\mathbf{x}_i \quad \mathbf{v}_i \quad \mathbf{b}_i]^T \quad (4)$$

where the 3D bias error of the accelerometer and gyroscope is 1D by combining the values of the 3-axes.

$$\mathbf{b}_i = [b_{\text{acc},i} \quad b_{\text{gyro},i}] \quad (5)$$

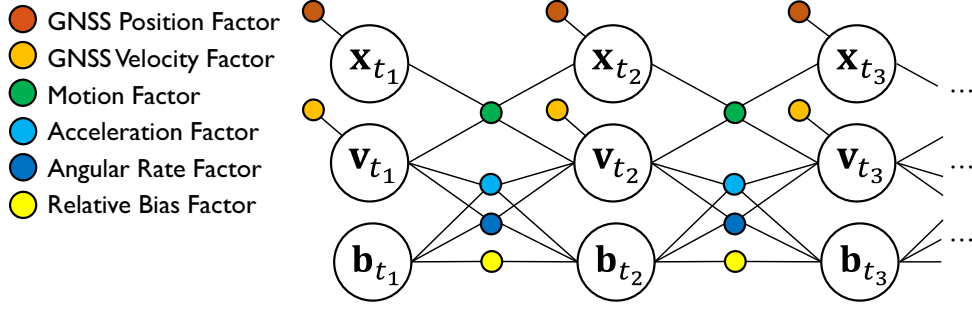


Fig. 1. Structure of the factor graph of the proposed method. The states are 3D position \mathbf{x} , velocity \mathbf{v} , and IMU bias \mathbf{b} ; attitude is not included in the states. IMU acceleration and angular velocity factors create a constraint between successive velocities.

By applying the constraints obtained from the IMU measurements between the above states, the GNSS and IMU are combined to improve position estimation accuracy.

C. Graph Structure

This study uses factor graph optimization (FGO) to estimate position by combining GNSS position and velocity, IMU acceleration, and angular velocity. A factor graph is a graphical representation of the constraints of a variable node expressed in edges between the variable node and the factor node [25].

The graph structure of the proposed method is shown in Fig. 1. The graph is constructed with GNSS observation timing (1 Hz), which is lower rate than IMU (100 Hz). We propose two new factors: (1) a constraint on the magnitude of the 3D acceleration vector and (2) an angular rate constraint between velocity vectors based on angle change. These IMU-based constraints are independent of attitude and do not require attitude to be added to the state. In addition, we also use a motion factor that relates velocity to position, a GNSS position factor that is a 3D position constraint using GNSS pseudorange, and a GNSS velocity factor that is a 3D velocity constraint using Doppler measurements.

D. Acceleration Factor

The acceleration factor constrains the change of successive 3D velocities using the magnitude of the 3D acceleration measurement from the accelerometer. Let the time of the i -th epoch be t_1 and the time of the $i+1$ -th epoch be t_2 , the error function of the acceleration factor is defined as

$$e_{\text{acc},i} = \left\| \frac{\mathbf{v}_{i+1} - \mathbf{v}_i}{\Delta t_{\text{gnss}}} - \mathbf{g} \right\| - \left\| \frac{\Delta t_{\text{imu}}}{\Delta t_{\text{gnss}}} \sum_{t=t_1}^{t_2} \mathbf{a}_t \right\| + b_{\text{acc},i} \quad (6)$$

where Δt_{gnss} and Δt_{imu} are the observation time step for GNSS and IMU, respectively. The first term represents the magnitude of the acceleration computed from velocities, and the second term represents the magnitude of the average acceleration between states calculated from the accelerometers. It is clear from this equation that by using only the magnitude of the 3D acceleration vector as a constraint, a constraint between states \mathbf{v}_i and \mathbf{v}_{i+1} can be constructed that is independent of the IMU's attitude. The total minimized error of the acceleration factor is calculated as:

$$\|e_{\text{acc},i}\|_{\Omega_{\text{acc}}} = e_{\text{acc},i} \Omega_{\text{acc}} e_{\text{acc},i} \quad (7)$$

where Ω_{acc} is the information matrix, which is empirically determined from the catalog-specified noise model of acceleration.

E. Angular Velocity Factor

The direction of the 3D velocity vector is constrained by the observed angular velocity of a gyroscope. This can be expressed as the constraint that the angle formed by the velocity vectors between successive states coincides with the angular change resulting from the integration of the angular velocity measurements from the gyroscope. The error function of the angular velocity factor is defined as

$$e_{\text{gyro},i} = \arccos \left(\frac{\mathbf{v}_{i+1} \cdot \mathbf{v}_i}{\|\mathbf{v}_{i+1}\| \|\mathbf{v}_i\|} \right) - \left\| \sum_{t=t_1}^{t_2} \omega_t \Delta t_{\text{imu}} \right\| + b_{\text{gyro},i} \quad (8)$$

This equation expresses the constraint that the angle between the velocity vectors is equal to the angular change due to the integration of the angular velocity. The error function to be optimized is as follows

$$\|e_{\text{gyro},i}\|_{\Omega_{\text{gyro}}} = e_{\text{gyro},i} \Omega_{\text{gyro}} e_{\text{gyro},i} \quad (9)$$

where Ω_{gyro} is the information matrix, which is empirically determined from the gyroscope specifications as well as the accelerometer. This angular velocity constraint is valid in vehicles and robots, where nonholonomic models can be applied. In addition, this constraint cannot be used when the velocity is zero or the velocity is small. Therefore, this constraint is only applied when the magnitude of the velocity vector exceeds a certain threshold (1 m/s in this paper).

F. Other Factors

1) *GNSS Position Factor*: The 3D positioning results from the least-squares method using GNSS pseudorange are combined for position estimation. The error function of the GNSS position factor is

$$\mathbf{e}_{\text{pos},i} = \mathbf{x}_i - \mathbf{x}_{\text{gnss},i} \quad (10)$$

where, $\mathbf{x}_{\text{gnss},i}$ is the GNSS positioning solution in the ENU coordinate system. The information matrix of the GNSS

position factor is computed from the covariance matrix estimated by the least-squares method.

2) *GNSS Velocity Factor*: The 3D velocity is estimated by the least squares method using the GNSS Doppler shift measurements. As with the position factor, the 3D velocity $\mathbf{v}_{\text{gnss},i}$ is converted to the ENU coordinate system and added to the graph as follows.

$$\mathbf{e}_{\text{vel},i} = \mathbf{v}_i - \mathbf{v}_{\text{gnss},i} \quad (11)$$

As with the position factor, the covariance matrix estimated by the least squares method is used to compute the information matrix. In general, the velocity calculated from the Doppler velocity is much more accurate than the velocity calculated from the difference of pseudoranges, and combining the Doppler velocity with position estimation allows for higher accuracy and robustness.

3) *Motion Factor*: The motion factor is used to relate 3D velocity and position. The motion factor is defined as follows based on the average velocity and 3D position between successive states.

$$\mathbf{e}_{\text{m},i} = \frac{\mathbf{x}_{i+1} - \mathbf{x}_i}{\Delta t_{\text{gnss}}} - \frac{\mathbf{v}_{i+1} + \mathbf{v}_i}{2} \quad (12)$$

By using the motion factor, the acceleration and angular velocity constraints between velocities are also propagated to the position, improving the position estimation accuracy.

4) *Relative Bias Factor*: The relative bias factor between IMU bias states is used to control the variation of the acceleration and angular velocity bias errors. The following equations define the error functions for the relative bias factor.

$$e_{\text{bias},a,i} = b_{\text{acc},i+1} - b_{\text{acc},i} \quad (13)$$

$$e_{\text{bias},g,i} = b_{\text{gyro},i+1} - b_{\text{gyro},i} \quad (14)$$

where the information matrix of the relative bias factor is determined from the random walk specifications of the accelerometer and gyroscope.

G. Optimization

The final objective function to be optimized is expressed by the following equation.

$$\begin{aligned} \hat{\mathbf{X}} = \underset{\mathbf{X}}{\text{argmin}} & \sum_i \|e_{\text{acc},i}\|_{\Omega_{\text{acc}}}^2 + \sum_i \|e_{\text{gyro},i}\|_{\Omega_{\text{gyro}}}^2 \\ & + \sum_i \|\mathbf{e}_{\text{pos},i}\|_{\Omega_{\text{pos},i}}^2 + \sum_i \|\mathbf{e}_{\text{vel},i}\|_{\Omega_{\text{vel},i}}^2 + \sum_i \|\mathbf{e}_{\text{m},i}\|_{\Omega_{\text{m}}}^2 \\ & + \sum_i \|e_{\text{bias},a,i}\|_{\Omega_{\text{bias},a}}^2 + \sum_i \|e_{\text{bias},g,i}\|_{\Omega_{\text{bias},g}}^2 \end{aligned} \quad (15)$$

There are several ways to use the proposed method for real-time position estimation applications, including partial optimization using sliding windows and iSAM [26]. In this paper, we treat the optimization as a whole graph optimization problem using the Levenberg-Marquardt optimizer as a post-processing application. For the GNSS position and

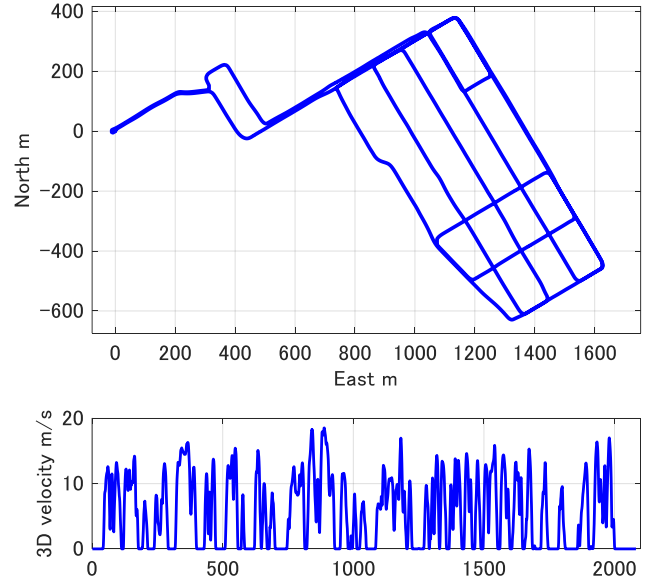


Fig. 2. Trajectory (top) and 3D velocity history (bottom) of the simulation data. The data was generated from the vehicle's urban driving data.

TABLE I
SENSOR PARAMETERS FOR IMU AND GNSS DATA SIMULATION.

| Sensor | Parameter | Value | Unit |
|---------------|---------------|-----------------------|-----------------------------------|
| Acceleration | Noise density | 1.86×10^{-3} | $(\text{m/s}^2)/\sqrt{\text{Hz}}$ |
| | Random walk | 4.33×10^{-4} | $(\text{m/s}^2)\sqrt{\text{Hz}}$ |
| | Constant bias | 0.19 | m/s^2 |
| | Sample rate | 100 | Hz |
| Angular rate | Noise density | 1.87×10^{-4} | Unit |
| | Random walk | 2.66×10^{-5} | $(\text{rad/s})/\sqrt{\text{Hz}}$ |
| | Constant bias | 0.0545 | $(\text{rad/s})\sqrt{\text{Hz}}$ |
| | Sample rate | 100 | rad/s |
| GNSS position | Noise density | 1.0 | m |
| | Sample rate | 1 | Hz |
| GNSS velocity | Noise density | 0.2 | m/s |
| | Sample rate | 1 | Hz |

velocity error functions, the M-estimator is applied as a robust optimization method due to the existence of outliers caused by multipath. The Huber function is used as the kernel [27]. GTSAM, a general-purpose graph optimization library, is used to implement the proposed method [28]. As described above, the proposed method does not estimate the attitude, but estimates the 3D position by combining the IMU and GNSS observations.

III. EXPERIMENTS

We compare the proposed method with the conventional general 6-DOF GNSS/IMU integration method. As an implementation of the 6-DOF GNSS/IMU integration method, we use the GNSS/IMU integration algorithm based on graph-based optimization using GTSAM. It uses the IMU preintegration factor as the IMU constraint [29], [30], and the estimated state is a 15-dimensional vector, including the 3D attitude shown in equation (1). The proposed method and

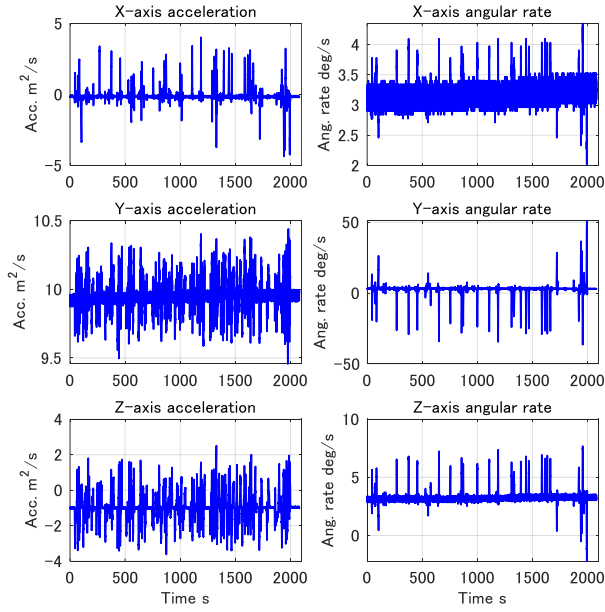


Fig. 3. IMU acceleration and angular velocity data generated from driving scenarios. IMU mounting angles are matched to data from actual driving experiments.

the comparison method differ only in the graph structure of the IMU part; the rest of the graph by GNSS is the same, and similar parameters are used. We evaluate the proposed method using two datasets: simulation data and real data obtained by placing a smartphone on a vehicle.

A. Simulation Setup

Simulation data of IMU and GNSS observations were generated to evaluate the position estimation performance of the proposed method. MATLAB Navigation Toolbox was used to generate simulation data for IMU and GNSS. As the vehicle trajectory for generating sensor data, we used the vehicle trajectory from the Google Smartphone Decimeter Challenge [31], an evaluation using real data described below, to generate GNSS and IMU observation data.

Fig. 2 shows the trajectory and 3D velocity of the vehicle in the simulation data. The travel distance is approximately 12 km, including vehicle stops and starts in an urban environment, and takes approximately 35 minutes.

Fig. 3 shows the generated IMU measurements (acceleration and angular velocity). The parameters of the sensor models used to generate the simulation data are listed in Table I. Parameters such as accelerometer, gyroscope noise density, and random walk were set using parameter estimates from low-cost IMUs based on the reference [32]. GNSS observations were generated by adding Gaussian noise to 3D position and 3D velocity. The noise of the GNSS velocity observation is set lower than that of the position observation. IMU measurements were generated at 100 Hz, and GNSS observations were generated at 1 Hz.

Several simulation data were generated with errors added to the IMU mounting position to compare the proposed and conventional methods. The parameters required for the

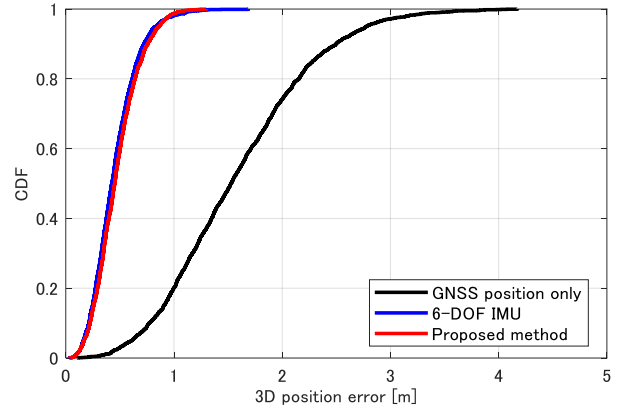


Fig. 4. Cumulative distribution function of 3D position error for the proposed (red line) and conventional 6-DOF pose estimation (blue line). The combined IMU significantly improves the accuracy of position estimation in both cases.

TABLE II

RMS POSITION ERROR BETWEEN THE PROPOSED METHOD AND CONVENTIONAL 6-DOF ATTITUDE ESTIMATION IN SIMULATION DATA.

| | East error m | North error m | Up error m | 3D position error m |
|--------------------|--------------|---------------|------------|---------------------|
| GNSS position only | 1.003 | 0.990 | 0.997 | 1.726 |
| 6-DOF IMU | 0.293 | 0.260 | 0.310 | 0.499 |
| Proposed method | 0.327 | 0.299 | 0.265 | 0.516 |

proposed and conventional methods, such as the information matrix in the graph optimization, are assumed to be known. The same parameters as those used to generate the IMU and GNSS data by simulation are used in the evaluation.

B. Comparison by IMU Mounting Position Error

Fig. 4 shows the cumulative distribution function of 3D position error for the proposed (red line) and conventional 6-DOF pose estimation (blue line). Both the proposed and conventional methods improve the accuracy of position estimation by combining IMUs. Table II shows the root means square (RMS) errors of estimated position for each method.

When there is no IMU mounting position error (when the IMU frame is coincident with the vehicle frame), the proposed method improves the estimation accuracy, but the position estimation accuracy is slightly lower than that of the conventional method. This is because the conventional method can ideally integrate the GNSS and IMU under the condition that the sensor model parameters are known. In addition, the proposed method does not maximize the use of the IMU's 3-axis observations and limits the observations, which degrades the performance compared to the case where the full acceleration and angular velocity observations are used.

Fig. 5 shows the RMS error in 3D position estimation when a constant IMU mounting position error from the vehicle frame origin is added to the x -axis. As shown in Fig. 5, the position estimation accuracy of the proposed method is less affected by the IMU mounting position. However, the conventional method, a 6-DOF pose estimation method, shows that the accuracy of the position estimation decreases

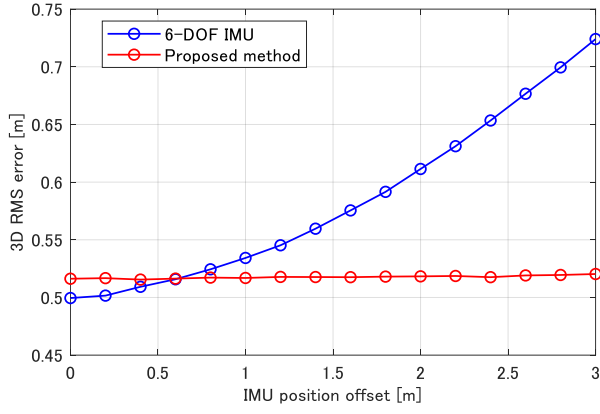


Fig. 5. Comparison of position estimation error with increasing IMU mounting position error. The proposed method (red line) is less sensitive to the IMU mounting position error, while the conventional 6-DOF pose estimation (blue line) has an increasing error.

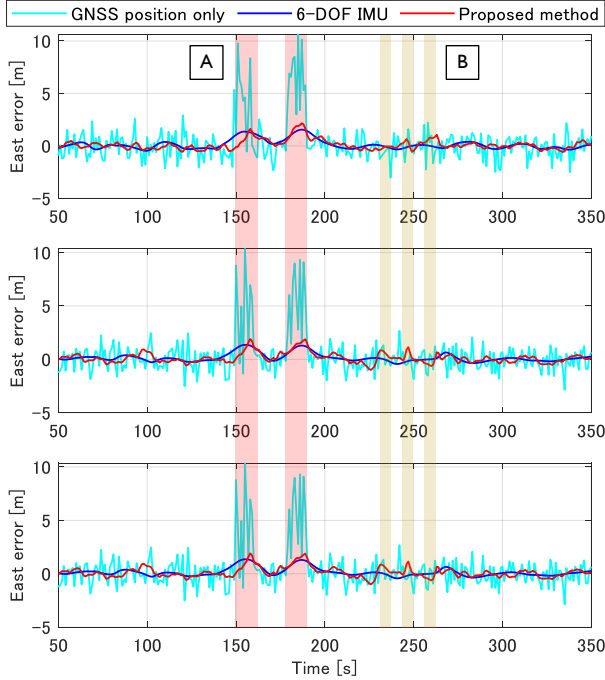


Fig. 6. Position estimation errors of the proposed method (red line) and the conventional method (blue line) when multipath is included in GNSS observations (A) and when GNSS observations are missing (B).

as the IMU mounting position error increases.

When the IMU mounting position error exceeds 0.6 m, the proposed method has better position estimation accuracy, and the advantage of the proposed method over the conventional method occurs. This is because the proposed method only considers the magnitude of the IMU's acceleration measurement. Thus the accuracy of the position estimation is less affected by the centripetal force. In contrast, the conventional 6-DOF pose estimation method is affected by the centripetal force acting on the IMU, which causes attitude estimation errors and simultaneously degrades the position estimation accuracy.

C. Comparison by Multipath and GNSS Shielding

We evaluate the degradation of the position estimation accuracy of each method by simulating the case where the GNSS observations have large position and velocity errors due to multipath and another case where the satellite has a short time loss due to shielding. Fig. 6 shows the position estimation errors for the case without IMU, 6-DOF pose estimation, and the proposed method. The section "A" is a randomly observed position and velocity with errors added by simulating multipath. In the case without IMU, the position estimation accuracy in section "A" is significantly degraded due to multipath. The combined use of the IMU and the proposed method significantly reduces the estimation error for both the proposed and conventional methods.

In section "B", even when GNSS signals are not available, the position can be calculated using IMU, and it can be confirmed that both the proposed and conventional methods can suppress the increase in position estimation error. The proposed method can improve the accuracy of position estimation even when the GNSS observation data contains errors and deficiencies by combining GNSS and IMU without estimating the attitude.

D. Actual Smartphone Dataset

GNSS and IMU data collected in a real-world environment were used to evaluate the proposed method. The Google Smartphone Decimeter Challenge dataset [31] is used for the evaluation. In this dataset, a smartphone is mounted on a vehicle's dashboard, and data is collected from the smartphone's built-in GNSS and IMU. The mounting position and orientation of the smartphone were not provided. For the evaluation in this paper, the smartphone is assumed to be installed at the origin of the vehicle frame and is used to evaluate the combined GNSS and IMU.

The vehicle trajectories are the same as those used to generate the simulation data, and the evaluation is performed on multiple trajectories measured at different dates and times. Fig. 7 shows the driving trajectory of a vehicle equipped with a smartphone. The driving environment is an urban environment lined with buildings with large multipath errors, where GNSS is completely blocked for several seconds by tall structures and buildings, making it difficult to achieve high-accuracy positioning using GNSS alone.

The IMU data observed by the smartphone is very noisy and has many missing and abnormal values. The sampling period is not constant and varies between 50 Hz and 100 Hz. The IMU and GNSS of smartphones also have the problem of observation time offset. In this study, fixed value time offsets between GNSS and IMU were manually estimated and applied [33]. Parameters such as IMU noise were manually tuned for both the proposed and conventional methods.

The GNSS 3D position observations are based on the position information contained in the dataset estimated by the weighted least squares method using the pseudorange from the raw GNSS data of the smartphone. The 3D velocity

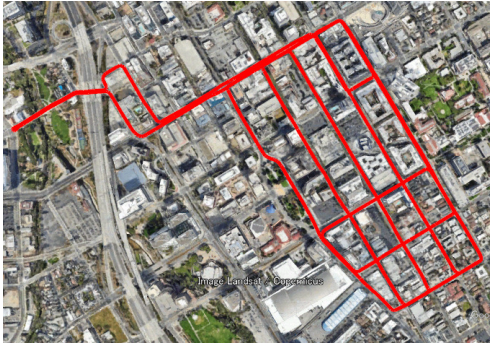


Fig. 7. Driving trajectory of a vehicle equipped with a smartphone. The experimental environment is a downtown area, where GNSS signal shielding and multipath occur frequently.

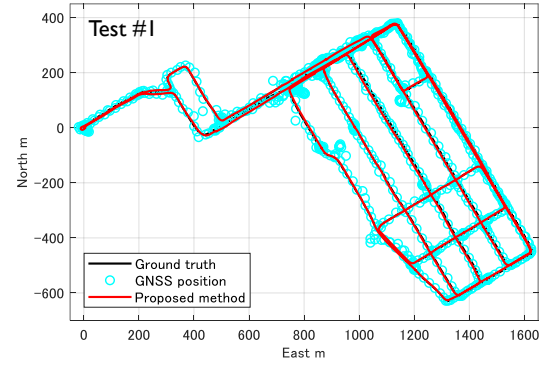


Fig. 8. The position estimation results using the proposed method, where the combined use of IMUs provides smooth position estimation regardless of GNSS errors and observation deficiencies.

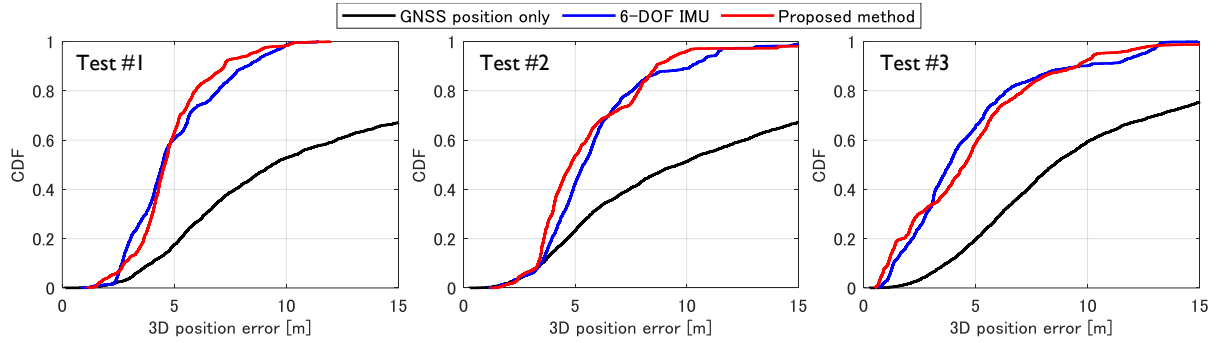


Fig. 9. Comparison of the cumulative distribution function of the proposed method (red line) and the conventional method (blue line) for three vehicle driving experiments. The proposed method shows slightly better performance than the conventional method.

TABLE III

RMS POSITION ERROR OF THE PROPOSED METHOD AND CONVENTIONAL 6-DOF POSE ESTIMATION IN ACTUAL SMARTPHONE DATASET.

| | Test #1 | | | | Test #2 | | | | Test #3 | | | |
|--------------------|--------------|---------------|------------|------------|--------------|---------------|------------|------------|--------------|---------------|------------|------------|
| | East error m | North error m | Up error m | 3D error m | East error m | North error m | Up error m | 3D error m | East error m | North error m | Up error m | 3D error m |
| GNSS position only | 8.671 | 11.228 | 23.808 | 27.714 | 9.698 | 10.495 | 22.782 | 26.893 | 11.920 | 9.179 | 15.506 | 21.605 |
| 6-DOF IMU | 3.674 | 2.448 | 3.133 | 5.413 | 4.752 | 3.050 | 3.239 | 6.510 | 3.976 | 2.860 | 2.804 | 5.643 |
| Proposed method | 3.815 | 2.754 | 2.075 | 5.143 | 5.008 | 3.078 | 2.253 | 6.295 | 3.900 | 3.060 | 3.063 | 5.827 |

data is estimated by the least squares method from the smartphone's Doppler observations.

Comparisons between the proposed and conventional methods were made for three sets of driving data collected on different dates. Fig. 8 shows an example of a smartphone trajectory estimated by the proposed method; although the GNSS position contains a very large positioning error due to multipath, the proposed method is able to estimate a smooth trajectory by combining IMUs. Fig. 9 shows the comparison of the cumulative distribution function of the proposed method (red line) and the conventional method (blue line) for three vehicle driving experiments. Table III shows the RMS error of 3D position estimation. Both the proposed method and the conventional method can estimate a smooth position without increasing the error, even in areas where the GNSS pseudorange-based position has large errors in the observations, by combining the IMU. The proposed method and the conventional method showed almost the same level of position estimation performance, and better

performance than the conventional method for some runs. This is thought to be due to the influence of mounting errors and the fact that the IMU data acquired in the real environment was degraded by noise and vibration.

IV. CONCLUSION

In this study, we proposed a combined GNSS and IMU method that does not require attitude estimation. In the state estimation problem by graph optimization, we proposed a constraint between states using the magnitude of the 3D acceleration vector observed by the IMU and a constraint of the angle of the velocity vector between states using the angle change by the gyroscope observation values and conducted an evaluation using simulation data and smartphone observation in a real environment. In the evaluation with simulation data, it was shown that the proposed method improves the position estimation accuracy by combining IMUs even when there are large errors or deficiencies in the GNSS observations. It was also confirmed that the proposed

method is not significantly affected by the IMU mounting position, and the position estimation accuracy does not deteriorate when there are errors in the IMU mounting position, while the conventional 6-DoF estimation method deteriorates the position estimation accuracy. In the real-world position estimation of smartphones, the proposed method improves positioning accuracy by combining IMUs. In conclusion, the proposed method is highly effective in the combined GNSS and IMU scenario where the IMU is frequently installed and removed.

In this paper, we evaluate the performance of the proposed method by integrating loose-coupled GNSS position and velocity with IMU. In the future, we will improve the position estimation performance by evaluating the combination of IMU with tight-coupling GNSS pseudorange and Doppler, and by combining more advanced velocity information such as time-differenced carrier phase.

REFERENCES

- [1] P. Misra and P. Enge, "Global positioning system: Signals, measurements and performance second edition."
- [2] E. D. Kaplan and C. Hegarty, *Understanding GPS/GNSS: principles and applications*. Artech house, 2017.
- [3] P. J. Teunissen and O. Montenbruck, *Springer handbook of global navigation satellite systems*. Springer, 2017, vol. 10.
- [4] L. Serrano, D. Kim, R. B. Langley, K. Itani, and M. Ueno, "A GPS velocity sensor: How accurate can it be? - A first look," in *Proceedings of the National Technical Meeting, Institute of Navigation*, vol. 2004, 2004, pp. 875–885.
- [5] N. Kubo, "Advantage of velocity measurements on instantaneous rtk positioning," *GPS solutions*, vol. 13, no. 4, pp. 271–280, 2009.
- [6] P. D. Groves, *Principles of GNSS, Inertial, and Multisensor Integrated Navigation Systems*. Norwood, MA, USA: Artech House, 2013.
- [7] S. Madgwick *et al.*, "An efficient orientation filter for inertial and inertial/magnetic sensor arrays," *Report x-io and University of Bristol (UK)*, vol. 25, pp. 113–118, 2010.
- [8] W. Xiwei, X. Bing, W. Cihang, G. Yiming, and L. Lingwei, "Factor graph based navigation and positioning for control system design: A review," *Chinese Journal of Aeronautics*, vol. 35, no. 5, pp. 25–39, 2022.
- [9] Z. Gong, R. Ying, F. Wen, J. Qian, and P. Liu, "Tightly coupled integration of gnss and vision slam using 10-dof optimization on manifold," *IEEE Sensors Journal*, vol. 19, no. 24, pp. 12 105–12 117, 2019.
- [10] T. Qin, S. Cao, J. Pan, and S. Shen, "A general optimization-based framework for global pose estimation with multiple sensors," *arXiv preprint arXiv:1901.03642*, 2019.
- [11] L. Chang, X. Niu, T. Liu, J. Tang, and C. Qian, "Gnss/ins/lidar-slam integrated navigation system based on graph optimization," *Remote Sensing*, vol. 11, no. 9, 2019. [Online]. Available: <https://www.mdpi.com/2072-4292/11/9/1009>
- [12] H. Chen, W. Wu, S. Zhang, C. Wu, and R. Zhong, "A gnss/lidar/imu pose estimation system based on collaborative fusion of factor map and filtering," *Remote Sensing*, vol. 15, no. 3, 2023. [Online]. Available: <https://www.mdpi.com/2072-4292/15/3/790>
- [13] A. Stateczny, C. Specht, M. Specht, D. Brčić, A. Jugović, S. Wiśniewski, M. Wiśniewska, and O. Lewicka, "Study on the positioning accuracy of gnss/ins systems supported by dgps and rtk receivers for hydrographic surveys," *Energies*, vol. 14, no. 21, p. 7413, 2021.
- [14] H. Qi and J. B. Moore, "Direct kalman filtering approach for gps/ins integration," *IEEE Transactions on Aerospace and Electronic Systems*, vol. 38, no. 2, pp. 687–693, 2002.
- [15] W. Ding, J. Wang, C. Rizos, and D. Kinlyside, "Improving adaptive kalman estimation in gps/ins integration," *The Journal of Navigation*, vol. 60, no. 3, pp. 517–529, 2007.
- [16] V. Indelman, S. Williams, M. Kaess, and F. Dellaert, "Factor graph based incremental smoothing in inertial navigation systems," in *2012 15th International Conference on Information Fusion*, 2012, pp. 2154–2161.
- [17] W. Li, X. Cui, and M. Lu, "A robust graph optimization realization of tightly coupled gnss/ins integrated navigation system for urban vehicles," *Tsinghua Science and Technology*, vol. 23, no. 6, pp. 724–732, 2018.
- [18] G. Wang, X. Xu, J. Wang, and Y. Zhu, "An enhanced ins/gnss tightly coupled navigation system using time-differenced carrier phase measurement," *IEEE Transactions on Instrumentation and Measurement*, vol. 69, no. 7, pp. 5208–5218, 2019.
- [19] W. Wen, X. Bai, Y. C. Kan, and L.-T. Hsu, "Tightly coupled gnss/ins integration via factor graph and aided by fish-eye camera," *IEEE Transactions on Vehicular Technology*, vol. 68, no. 11, pp. 10 651–10 662, 2019.
- [20] P. Lyu, S. Bai, J. Lai, B. Wang, X. Sun, and K. Huang, "Optimal time difference-based tdcg-gps/imu navigation using graph optimization," *IEEE Transactions on Instrumentation and Measurement*, vol. 70, pp. 1–10, 2021.
- [21] W. Wen, T. Pfeifer, X. Bai, and L.-T. Hsu, "Factor graph optimization for gnss/ins integration: A comparison with the extended kalman filter," *NAVIGATION*, vol. 68, no. 2, pp. 315–331, 2021. [Online]. Available: <https://onlinelibrary.wiley.com/doi/abs/10.1002/navi.421>
- [22] C. Kilic, S. Das, E. Gutierrez, R. Watson, and J. Gross, "Zupt aided gnss factor graph with inertial navigation integration for wheeled robots," in *Proceedings of the 34th International Technical Meeting of the Satellite Division of The Institute of Navigation (ION GNSS+ 2021)*, 2021, pp. 3285–3293.
- [23] Z. F. Syed, P. Aggarwal, X. Niu, and N. El-Sheimy, "Civilian vehicle navigation: Required alignment of the inertial sensors for acceptable navigation accuracies," *IEEE Transactions on Vehicular Technology*, vol. 57, no. 6, pp. 3402–3412, 2008.
- [24] Z. Bao, G. Lu, Y. Wang, and D. Tian, "A calibration method for misalignment angle of vehicle-mounted imu," *Procedia - Social and Behavioral Sciences*, vol. 96, pp. 1853–1860, 2013, intelligent and Integrated Sustainable Multimodal Transportation Systems Proceedings from the 13th COTA International Conference of Transportation Professionals (CICTP2013). [Online]. Available: <https://www.sciencedirect.com/science/article/pii/S1877042813023367>
- [25] F. Dellaert, "Factor Graphs and GTSAM: A Hands-on Introduction," Tech. Rep., 2012.
- [26] M. Kaess, A. Ranganathan, and F. Dellaert, "isam: Incremental smoothing and mapping," *IEEE Transactions on Robotics*, vol. 24, no. 6, pp. 1365–1378, 2008.
- [27] X. Bai, W. Wen, and L.-T. Hsu, "Time-correlated window-carrier-phase-aided gnss positioning using factor graph optimization for urban positioning," *IEEE Transactions on Aerospace and Electronic Systems*, vol. 58, no. 4, pp. 3370–3384, 2022.
- [28] F. Dellaert and G. Contributors, "borglab/gtsam," May 2022. [Online]. Available: <https://github.com/borglab/gtsam>
- [29] T. Lupton and S. Sukkarieh, "Visual-inertial-aided navigation for high-dynamic motion in built environments without initial conditions," *IEEE Transactions on Robotics*, vol. 28, no. 1, pp. 61–76, 2012.
- [30] C. Forster, L. Carlone, F. Dellaert, and D. Scaramuzza, "Imu preintegration on manifold for efficient visual-inertial maximum-a-posteriori estimation," Georgia Institute of Technology, 2015.
- [31] G. M. Fu, M. Khider, and F. van Diggelen, "Android raw gnss measurement datasets for precise positioning," in *Proceedings of the 33rd International Technical Meeting of the Satellite Division of The Institute of Navigation (ION GNSS+ 2020)*, 2020, pp. 1925–1937.
- [32] J. Rehder, J. Nikolic, T. Schneider, T. Hinzmann, and R. Siegwart, "Extending kalibr: Calibrating the extrinsics of multiple imus and of individual axes," in *2016 IEEE International Conference on Robotics and Automation (ICRA)*, 2016, pp. 4304–4311.
- [33] H. Sharma, M. Bochkati, and T. Pany, "Time-synchronized gnss/imu data logging from android smartphone and its influence on the positioning accuracy," in *Proceedings of the 34th International Technical Meeting of the Satellite Division of The Institute of Navigation (ION GNSS+ 2021)*, 09 2021.